



Research Paper

Cite this article: Kumar S, Ram G, Mandal D, Kar R (2024) Optimal pattern synthesis of circular antenna arrays with improved effective aperture and beam area. *International Journal of Microwave and Wireless Technologies* 16(5), 871–884. <https://doi.org/10.1017/S1759078723001617>


Received: 9 July 2023
Revised: 2 December 2023
Accepted: 11 December 2023

Keywords:

beam area; circular antenna array; directivity; FNBW; novel particle swarm optimization; SLL

Corresponding author: Gopi Ram;
Email: gopi.ram@nitw.ac.in

Optimal pattern synthesis of circular antenna arrays with improved effective aperture and beam area

Satish Kumar, Gopi Ram , Durbadal Mandal and Rajib Kar

Department of Electronics and Communication Engineering, National Institute of Technology Durgapur, West Bengal, India

Abstract

Circular antenna array (CAA) is one of the most widely used antenna array designs. This paper addresses the design challenges of the CAA with the non-uniform single ring, which is placed in an X-Y plane with the best sidelobe level (SLL) and improved first null beamwidth (FNBW). It has been solved using differential evolution, craziness-based particle swarm optimization (CRPSO), and novel particle swarm optimization (NPSO) techniques. An optimal combination of feeding current and inter-element spacing provides an array pattern with the best SLL and improved FNBW, as well as some other parameter calculations of the antenna array like maximum directivity, maximum effective aperture, total effective aperture, maximum beam area, total beam area, circumference, and radius of the CAAs using these techniques. There are six designs of CAAs with different antenna elements (i.e., 10-, 12-, 16-, 20-, 36-, and 64-elements) which have been taken into account. Simulations are done in MATLAB. Based on various simulation results, we can analyze the performance of SLL and FNBW with other parameters using NPSO and compare them with different techniques of CAAs, as shown in the numerical analysis and simulation result section.

Introduction

It is possible to design having a greater degree of freedom when asymmetric feeding current and non-uniform inter-element spacing are used [1]. The growing electromagnetic environment pollution has spurred the study of array pattern strategies, i.e., to reduce the sidelobe level (SLL) while maintaining the beamwidth. Circular antenna arrays (CAAs) have gained significant attention in wireless communication due to their ability to provide directional radiation patterns with high gain and low SLLs. The circular geometry of the array ensures uniform distribution of power in all directions [2], making it ideal for applications requiring omnidirectional coverage, such as satellite communication, mobile networks, and radar systems for minimizing performance loss in the signal-to-noise ratio caused by unwanted interference [3]. Equally spaced, uniformly stimulated antenna arrays [4, 5] have good directivity but frequently have high SLL. To reduce the SLL, optimize the inter-element spacing and excitation amplitude of the arrays' elements.

In recent years, CAAs have been extensively studied to improve their performance regarding radiation patterns, beamforming, polarization diversity, and bandwidth of different antenna arrays. To address the demand for long-distance communication in various applications, constructing antennas with very directional properties is required. An antenna array combines radiating elements in an electrical and geometrical configuration. The total field of the antenna array is calculated by adding the fields emitted by each component vectorially [6]. Each element is positioned along the circle's perimeter in a circular array. As opposed to other array shapes, circular arrays have gained popularity recently since they can execute scans in all directions without significantly changing the beam pattern and offer 360° azimuth coverage. Additionally, because they lack edge elements, compared circular arrays to linear and rectangular arrays, they are less susceptible to mutual coupling [7].

The first metaheuristic technique has been deployed towards the CAA design problem in the work of Panduro *et al.* [8], who applied genetic algorithm (GA) to optimize the feeding current and between-element spacing of the CAAs' elements. Mohammad *et al.* [9] used the particle swarm optimization (PSO) technique and got better results than GA. Munish *et al.* [10] have applied simulated annealing (SA) for the same design problem and got better results as compared to the PSO technique. CAAs have also been used in radar systems, where they can provide high-resolution imaging and accurate target detection. In Tabesh *et al.*'s paper [11], a circular array was designed for radar applications, and the results showed that the array had improved resolution and sensitivity compared to traditional linear arrays. Ram *et al.* in paper [12] have used the seeker optimization

algorithm (SOA) to minimize the SLL of CAAs’ design problem. In addition, CAAs have been used in satellite communication systems, where they can provide reliable and high-speed data transmission. In paper [13], a circular array was used for satellite communication, and the results showed that the array had higher gain and lower noise levels than traditional linear arrays.

The primary goal of this article is to design CAAs with a small 3-dB beamwidth and low SLL. These two primary CAA design requirements are attained by selecting the optimum current amplitude excitation and inter-element spacing while maintaining a zero-phase difference between elements. Alberto *et al.* in paper [14] have discussed the approach to reducing SLL and the isoflux radiation requirement for geostationary Earth orbit (GEO) satellites using the PSO technique. The paper also discusses the challenges and future directions of research in concentric ring arrays (CRAs). Alberto *et al.* [15] also examined the concentric ring 61 disk patch antenna array for a reconfigurable isoflux pattern, including mutual coupling, using the cavity model at a frequency of 2.8 GHz. In this paper, harmony search algorithm (HSA) and PSO techniques are implemented in the optimization problem. In paper [16], Ibarra *et al.* designed a sparse CRA for isoflux coverage to the earth’s surface for the low Earth orbit satellite using optimization of the angular position of antenna elements and excitation amplitude. In paper [17], Ibarra *et al.* have also designed concentric ring antenna arrays (CRAAs) for GEO and medium Earth orbit satellites by getting isoflux radiation. In this paper, trade-off curves have been generated between SLL and isoflux mask error using the differential evolution (DE) technique. In paper [18], HSA and PSO techniques are implemented to get a wide coverage pattern of CRAA.

In this proposal, the variable used to alter the radiation pattern of both SLL and first null beamwidth (FNBW) with a maximum reduction is taken from the feeding current values and inter-element separations of the antenna elements using DE, CRPSO, and novel particle swarm optimization (NPSO) techniques. The NPSO technique is more efficient in improving directivity, effective aperture, and beam area problems for implementation in an application with a wide range.

The rest of the paper is arranged as follows: Mathematical formulation of CAA section presents the mathematical formulation of CAA. Formulation of fitness function section briefly discusses the formulation of the fitness function. In Optimization techniques employed section, the employed optimization technique has been discussed for the design of CAA. Numerical analysis and simulation results are explained in Section Numerical analysis and simulation results. Finally, concludes the paper.

Mathematical formulation of CAA

A CAA is a group of single antenna elements with non-uniform or uniform spacing arranged circularly. The current feeding distribution and inter-element spacing are identical for all the radiating elements in uniform CAA. A non-uniform CAA, however, exhibits tapering distributions. The standard form of a circular array with the “N” number of elements in the X-Y plane with radius “a” and finding at a point P in the far field is shown in Fig. 1. The array radiation pattern may be mathematically represented by its array factor as [19] if the components of the CAA are conceived of as isotropic radiating sources.

$$AF(\theta, \varphi) = \sum_{n=1}^N I_n \cdot e^{j[\beta \cdot a \cdot \sin \theta \cdot \cos(\varphi - \varphi_n) + \alpha_n]} \quad (1)$$

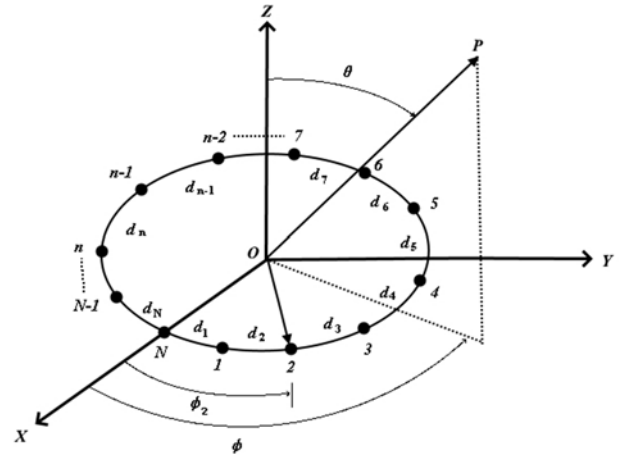


Figure 1. A non-uniform N-element CAA placed in X-Y plane with radius “a”.

where

I_n is the excitation amplitudes of the array, β is the propagation constant ($\beta = 2\pi/\lambda$), λ is the wavelength, θ indicates the incident angle of electromagnetic wave, ϕ is the azimuthal angle, φ_n is the angular position of the n th elements, α_n is the excitation phase of the n th elements.

$$\varphi_n = (2\pi/\beta a) \sum_{k=1}^n d_k \quad (2)$$

$$\alpha_n = -\beta \cdot a \cdot \cos(\varphi_0 - \varphi_n) \quad (3)$$

$$\beta \cdot a = \sum_{k=1}^n d_k = \frac{2\pi a}{\lambda} \quad (4)$$

After putting the value in Equation 1 from Equation 3, the total array factor can be as in Equation (5).

$$AF(\theta, \varphi) = \sum_{n=1}^N I_n \cdot e^{j \cdot \beta \cdot a \cdot [\sin \theta \cdot \cos(\varphi - \varphi_n) - \cos(\varphi_0 - \varphi_n)]} \quad (5)$$

where

$d = [d_1, d_2, d_3, \dots, d_N]$, and $I = [I_1, I_2, I_3, \dots, I_N]$. The excitation amplitude of n th elements and the distance from n th element to $(n + 1)$ th element are represented by I_n and d_n , respectively. In our design, at the most top radiation angle $\varphi_0 = 0^0$ in $\varphi = [-\pi, \pi]$, the global maximum is getting. To get the radiation pattern with the maximum reduction of SLL and improved FNBW in the preferred direction ϕ , the study’s goal is to choose the best combination of I_n and d_n values to modify the antenna design.

The directivity of CAAs is described by [15]

$$DIR = \frac{P(\theta, \varphi)}{\frac{1}{4\pi} \int_{4\pi} P(\theta, \varphi) d\Omega} \quad (6)$$

For a half-wave dipole antenna array, the effective aperture is given by [20]

$$A_{eff} = \frac{DIR \cdot \lambda^2}{4\pi} \quad (7)$$

The beam area is given by [21]

$$\Omega(sr) = \frac{4\pi}{DIR} \quad (8)$$

Table 1. Comparison of results obtained using the NPSO technique with other techniques for N = 10 elements

Algorithm	Optimal feeding current	Optimal inter-element spacing (in λ 's)	SLL (in dB)	FNBW (in degrees)
Uniform	1, 1, 1, 1, 1, 1, 1, 1, 1, 1	0.5, 0.5, 0.5, 0.5, 0.5, 0.5, 0.5, 0.5, 0.5, 0.5	-7.93	56.12
GA [8]	0.9545, 0.4283, 0.3392, 0.9074, 0.8086, 0.4533, 0.5634, 0.6015, 0.7045, 0.5948	0.3641, 0.4512, 0.2750, 1.6373, 0.6902, 0.9415, 0.4657, 0.2898, 0.6456, 0.3282	-9.811	NR
SA [10]	0.6920, 0.5679, 0.5937, 0.6703, 0.9693, 0.6014, 0.3575, 0.3020, 0.5908, 0.9718	0.6221, 0.9880, 0.7777, 0.9934, 0.6217, 0.9514, 0.7626, 0.5980, 0.7655, 0.9410	-13.00	NR
BBO [2]	1.0000, 1.0000, 1.0000, 0.3819, 0.8970, 1.0000, 0.7679, 0.8899, 0.7246, 1.0000	0.5301, 1.0603, 1.3264, 1.0000, 0.4307, 0.4408, 1.5276, 1.3255, 1.0000, 0.5904	-13.95	NR
SOA [12]	0.4472, 0.2924, 0.3356, 0.4214, 0.5818, 0.3783, 0.1824, 0.1508, 0.3818, 0.5722	0.6047, 0.9782, 0.7718, 0.9409, 0.6405, 0.9776, 0.7347, 0.5419, 0.7819, 0.9512	-12.83	NR
PSO [9]	1.0000, 0.7529, 0.7519, 1.0000, 0.5062, 1.0000, 0.7501, 0.7524, 1.0000, 0.5067	0.3170, 0.9654, 0.3859, 0.9654, 0.3185, 0.3164, 0.9657, 0.3862, 0.9650, 0.3174	-12.307	NR
OBA [27]	0.6563, 0.6619, 0.4060, 0.8677, 0.8310, 0.3194, 0.2825, 0.6239, 0.3901, 1.0000	0.5978, 1.6566, 0.8421, 1.7976, 0.5644, 1.5044, 0.7707, 1.2166, 1.0771, 0.6208	-14.06	NR
FA [28]	0.7081, 0.2682, 0.3713, 0.4100, 0.8800, 0.9665, 0.4165, 0.5813, 0.7494, 0.5403	0.3810, 0.7453, 0.2668, 0.3142, 1.0000, 0.6032, 0.9706, 0.5713, 0.8800, 0.3376	-13.30	NR
DE	0.7004, 0.5916, 0.6256, 0.7733, 0.9831, 0.5755, 0.5398, 0.5168, 0.6515, 0.8945	0.6562, 0.9968, 0.8365, 0.9556, 0.6041, 0.8807, 0.7934, 0.6291, 0.7713, 0.9540	-11.204	40.68
CRPSO	0.6396, 0.6569, 0.5174, 0.8279, 0.9794, 0.5972, 0.5413, 0.6297, 0.6317, 0.9269	0.6662, 0.9652, 0.8813, 0.9862, 0.5496, 0.8414, 0.8006, 0.6461, 0.7710, 0.9444	-11.810	39.96
NPSO	0.6187, 1.0000, 1.0000, 1.0000, 1.0000, 0.9931, 0.0000, 0.6751, 0.6749, 1.0000	0.6883, 0.8723, 0.8963, 0.5316, 0.5571, 0.5548, 0.5908, 0.8345, 0.5002, 0.5186	-14.140	48.24

NR* = not reported.

Table 2. Other parameters' comparison using NPSO technique with different algorithms for N = 10 elements

Algorithm	C; a (in λ 's)	DIR_max (in dB)	A_{eff_max} (in λ^2)	A_{eff_Total} (in λ^2)	Ω_{max} (in sr)	Ω_{total} (in sr)
Uniform	5; 0.7958	9.1169	0.6494	68.3737	1.5400	0.0146
DE	8.0777; 1.2856	10.6895	0.9327	57.7658	1.0722	0.0173
CRPSO	8.0520; 1.2815	10.6726	0.9291	58.8181	1.0763	0.0170
NPSO	6.5445; 1.0416	9.6415	0.7327	58.9401	1.3648	0.0170

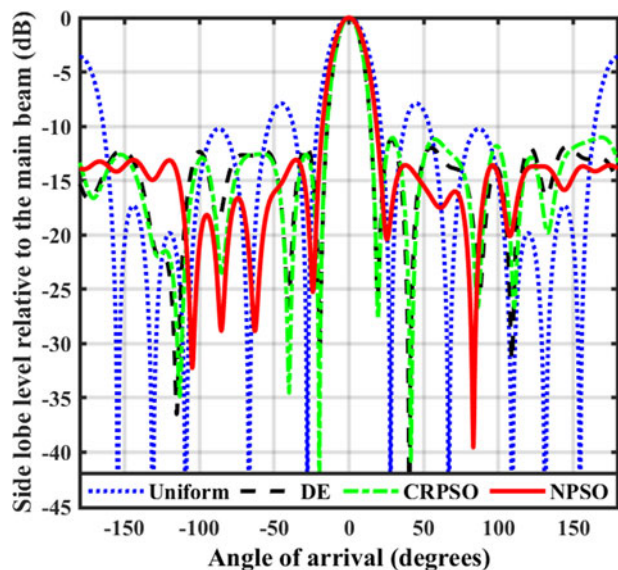


Figure 2. Radiation pattern of 10-element non-uniform CAAs.

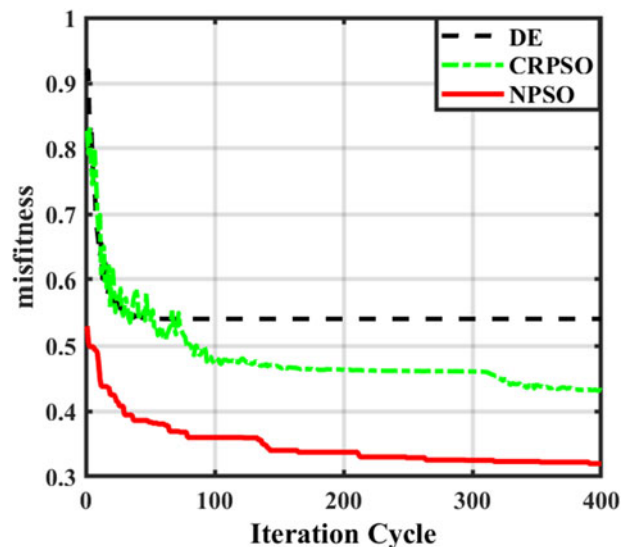


Figure 3. Convergence curve of 10-element non-uniform CAAs.

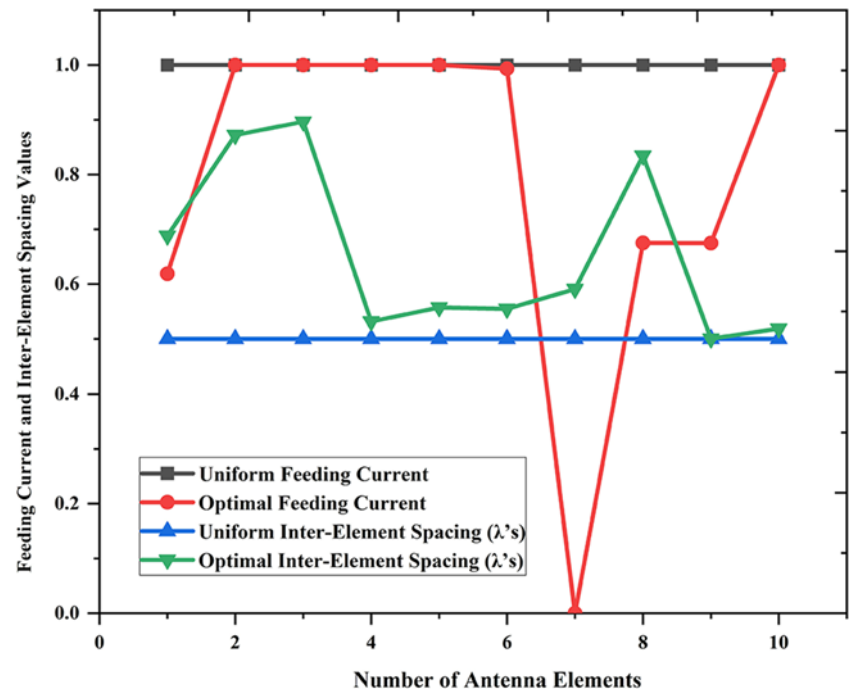


Figure 4. Optimal values of 10-element non-uniform CAAs using NPSO technique.

Table 3. Comparison of results obtained using the NPSO technique with other techniques for N = 12 elements

Algorithm	Optimal feeding current	Optimal inter-element spacing (in λ 's)	SLL (in dB)	FNBW (in degrees)
Uniform	1, 1, 1, 1, 1, 1, 1, 1, 1, 1, 1, 1	0.5, 0.5, 0.5, 0.5, 0.5, 0.5, 0.5, 0.5, 0.5, 0.5, 0.5, 0.5	-7.90	45.36
GA [8]	0.2064, 0.5416, 0.2246, 0.6486, 0.7212, 0.7913, 0.5277, 0.3495, 0.5125, 0.4475, 0.5233, 0.8553	0.4936, 0.4184, 1.4474, 0.7577, 0.4204, 0.5784, 0.4520, 0.8872, 0.7514, 0.4202, 0.4223, 0.7234	-11.830	NR
SA [10]	0.6231, 0.3990, 0.3418, 0.6054, 0.9444, 0.7380, 0.6741, 0.3001, 0.4311, 0.5435, 0.4195, 0.9795	0.8315, 0.7910, 0.6699, 0.8087, 0.7347, 0.5331, 0.4777, 0.8960, 0.4874, 0.8657, 0.3461, 0.5105	-13.910	NR
BBO [2]	1.0000, 0.6501, 0.6224, 0.5020, 0.5540, 1.0000, 0.6683, 0.7234, 0.4410, 0.5123, 0.4793, 1.0000	0.6704, 1.0000, 1.3046, 0.8081, 1.0000, 0.4031, 0.6183, 1.1574, 1.3465, 0.6551, 1.0000, 0.6539	-13.95	NR
SOA [12]	0.5169, 0.4519, 0.2006, 0.5273, 0.5617, 0.8967, 0.6691, 0.5912, 0.2432, 0.5839, 0.6416, 0.8285	0.8564, 0.8305, 0.6790, 0.5796, 0.8978, 0.7911, 0.5337, 0.9848, 0.7859, 0.8148, 0.9462, 0.5772	-13.77	NR
PSO [9]	0.9554, 0.6441, 0.7109, 0.7769, 1.0000, 1.0000, 0.3958, 0.7162, 0.6746, 0.7695, 0.9398, 0.6145	0.2569, 0.8509, 0.6607, 0.7057, 0.8540, 0.3734, 0.1609, 0.8321, 0.6464, 0.7079, 0.8330, 0.2682	-13.670	NR
OBA [27]	0.3930, 0.3897, 0.2555, 0.4092, 0.4450, 0.5533, 0.3088, 0.2993, 0.2579, 0.3854, 0.3732, 0.5210	0.6259, 1.0100, 0.7675, 1.3005, 1.3045, 0.5007, 0.4407, 0.9944, 0.7167, 0.7865, 1.5534, 0.6605	-14.30	NR
FA [28]	0.9175, 0.3153, 0.5814, 0.6311, 0.9629, 0.9903, 0.3297, 0.4345, 0.6820, 0.4397, 0.7151, 0.7605	0.3171, 0.8105, 0.5833, 0.7609, 0.8946, 0.4747, 0.9868, 0.2509, 0.2932, 0.7748, 0.6722, 0.3955	-14.21	NR
DE	0.7605, 0.7083, 0.6459, 0.8624, 0.5064, 0.9953, 0.6971, 0.7033, 0.2115, 0.3643, 0.8801, 1.2868	0.8945, 0.7102, 0.6585, 0.7097, 0.8868, 0.7348, 0.5778, 1.0000, 0.7701, 0.7681, 0.9383, 0.5947	-11.610	36
CRPSO	0.6755, 0.6185, 0.5002, 0.5922, 0.7727, 0.9965, 0.5533, 0.5975, 0.5836, 0.6862, 0.5398, 0.9915	0.6253, 0.9885, 0.6666, 0.7771, 0.9989, 0.6410, 0.6110, 0.9393, 0.8000, 0.6305, 0.9911, 0.6830	-13.130	33.12
NPSO	0.5005, 0.5199, 0.2188, 0.4385, 0.2845, 0.9739, 0.7532, 0.1921, 0.4335, 0.7260, 0.9998, 0.8538	0.7844, 0.8035, 0.7091, 0.5683, 0.7578, 0.8808, 0.5417, 1.0000, 0.8575, 0.7863, 0.9738, 0.6519	-14.401	36.72

NR* = not reported.

Formulation of fitness function

The motivating factor of any optimization technique is the fitness or objective function. It is denoted as CF, given in Equation (9). The fitness or cost values of each solution string generated throughout

the search process are computed using it. In this design problem, each solution string represents different element excitation and inter-element spacing for different test cases. The objective is to design 8-, 10-, 12-, 16-, 20-, and 36-element CAAs with the

Table 4. Other parameters' comparison using NPSO technique with different algorithms for N = 12 elements

Algorithm	C; a (in λ's)	DIR_max (in dB)	A _{eff_max} (in λ ²)	A _{eff_Total} (in λ ²)	Ω_max (in sr)	Ω_total (in sr)
Uniform	6; 0.9549	9.6467	0.7336	61.6719	1.3631	0.0162
DE	9.2435; 1.4711	11.1392	1.0344	54.2279	0.9667	0.0184
CRPSO	9.3523; 1.4885	11.3996	1.0984	56.1913	0.9104	0.0178
NPSO	9.3151; 1.4825	11.1177	1.0293	55.7966	0.9715	0.0179

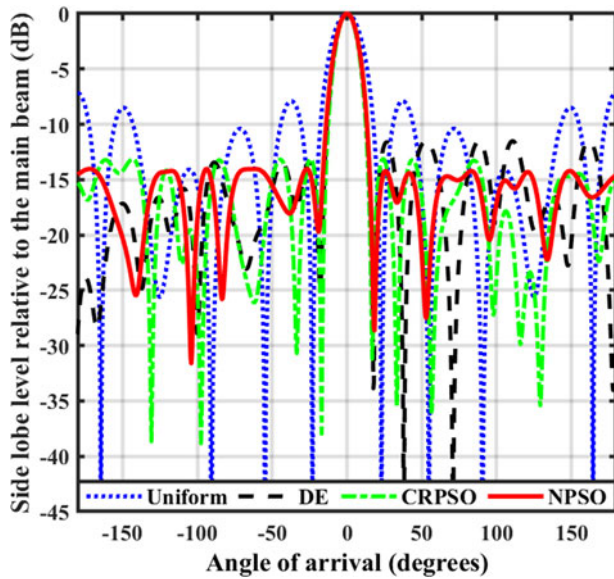


Figure 5. Radiation pattern of 12-element non-uniform CAAs.

lowest SLL, improved FNBW, and enhanced directivity. The fitness is designed as follows to achieve the ultimate goal:

$$CF = W_1 \times \frac{\prod_{\varphi=-180^\circ}^{LFN} |AF(\varphi_{sll}, I_n)|}{|AF(\varphi_0, I_n)|_{\max}} + W_2 \times \frac{\prod_{\varphi=RFN}^{180^\circ} |AF(\varphi_{sll}, I_n)|}{|AF(\varphi_0, I_n)|_{\max}} + W_3 \times |FNBW_0 - FNBW_R| + W_4 \times \frac{1}{DIR} + W_5 \times |C_0 - C_R| \quad (9)$$

where $C = \sum_{k=1}^N d_k$; d_k is the inter-element spacing [10].

$W_1, W_2, W_3, W_4,$ and W_5 are the weighted coefficients with equal values chosen, such as the optimal value of SLL remains more imposing than the optimal value of FNBW and CF never being negative. LFN is the left side of the first null, and RFN is the right side of the first null. φ_{sll} is the maximum SLL angle of the main beam side lobe on either side (i.e., LFN and RFN). $FNBW_0$ is the computed first null beamwidth in the non-uniform case, and $FNBW_R$ is the required first null beamwidth in the uniform case. $FNBW_0 < FNBW_R|_{I_n=1}$ condition must be satisfied to get an optimal set of feeding current and inter-element spacing otherwise discarded. DIR_{max} is the maximum directivity. C_0 is the computed circumference, and C_R is the required circumference.

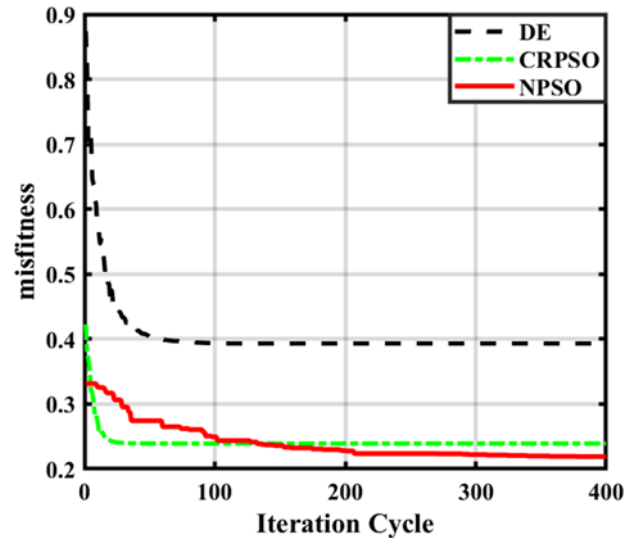


Figure 6. Convergence curve of 12-element non-uniform CAAs.

Optimization techniques employed

The DE and craziness-based particle swarm optimization (CRPSO) techniques are briefly discussed in papers [22] and [23], respectively. Therefore, the steps of DE and CRPSO are not discussed due to the space limitation. In the context of PSO, the velocity and position of the particle vector can be mathematically adjusted using the following equations, as described in papers [24–26].

$$V_i^{k+1} = w \times V_i^k + c_1 \times r_1 \times (pb_i^k - X_i^k) + c_2 \times r_2 \times (gb_i^k - X_i^k) \quad (11)$$

$$X_i^{k+1} = X_i^k + V_i^{k+1} \quad (12)$$

where ‘ r_1 ’ and ‘ r_2 ’ denote random values within the range of zero to one; The variables ‘ c_1 ’ and ‘ c_2 ’ represent the local acceleration and global acceleration constants of the particle, respectively. The symbol ‘ w ’ stands for a weighting factor; ‘ V_i^k ’ refers to the velocity of the i th particle in the k th iteration; ‘ pb_i^k ’ corresponds to the local best of the i th particle in the k th iteration; ‘ gb_i^k ’ signifies the global best among all particles in the k th iteration; lastly, ‘ X_i^k ’ pertains to the current position of the i th particle in the k th iteration.

When considering Equation (11), it is important to note that the two random values, r_1 and r_2 , are interrelated. If both of these random parameters have large values, it can lead to excessive reliance on individual and collective experiences, potentially causing the particle’s local optimum value to shift too far. On the other hand, if both r_1 and r_2 have small values, there is an incomplete utilization of individual and collective experiences, which, in turn, slows down the convergence speed of the optimization process.

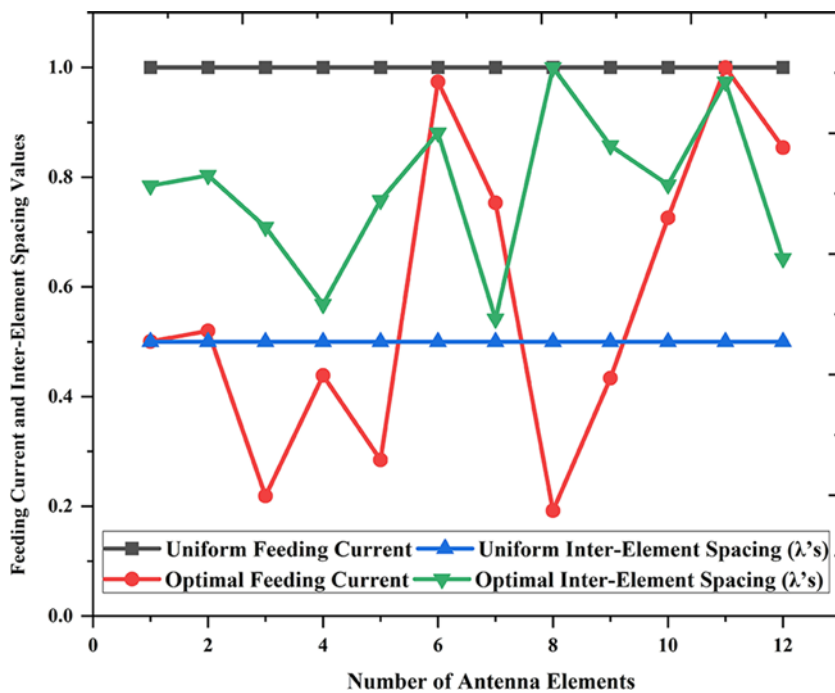


Figure 7. Optimal values of 12-element non-uniform CAAs using NPSO technique.

Table 5. Comparison of results obtained using the NPSO technique with other techniques for N = 16 elements

Algorithm	Optimal feeding current	Optimal inter-element spacing (in λ 's)	SLL (in dB)	FNBW (in degrees)
Uniform	1, 1, 1, 1, 1, 1, 1, 1, 1, 1, 1, 1, 1, 1, 1, 1	0.5, 0.5, 0.5, 0.5, 0.5, 0.5, 0.5, 0.5, 0.5, 0.5, 0.5, 0.5, 0.5, 0.5, 0.5	-7.94	34.56
DE	0.6372, 0.6649, 0.5003, 0.6558, 0.5107, 0.6372, 0.6348, 0.8146, 0.8118, 0.6014, 0.6228, 0.5002, 0.5859, 0.5615, 0.7163, 0.8904	0.6877, 0.8432, 0.7880, 0.6192, 0.6240, 0.8297, 0.7240, 0.6954, 0.5371, 0.7154, 0.9889, 0.8754, 0.7561, 0.9225, 0.5814, 0.5945	-11.926	27
CRPSO	0.4897, 0.4978, 0.5666, 0.3482, 0.5736, 0.5381, 0.2679, 0.6328, 1.0000, 0.5182, 0.4772, 0.3272, 0.6321, 0.5143, 0.8394, 0.9270	0.7018, 0.9595, 0.6122, 0.7522, 0.6645, 0.6844, 0.8784, 0.6470, 0.5787, 0.9487, 0.8382, 0.8207, 0.7841, 0.8310, 0.8485, 0.5044	-13.051	25.92
NPSO	0.6700, 0.5475, 0.5215, 0.5168, 0.6028, 0.5645, 0.5298, 0.7354, 0.9910, 0.8495, 0.5890, 0.6678, 0.6504, 0.5191, 0.9744, 0.9862	0.5157, 0.5367, 0.5552, 0.6160, 0.8198, 0.6126, 0.6412, 0.5508, 0.5077, 0.5018, 0.9131, 0.7877, 0.6905, 0.8021, 0.9726, 0.5173	-14.524	31.68

Table 6. Other parameters' comparison using NPSO technique with different algorithms for N = 16 elements

Algorithm	C_i ; a (in λ 's)	DIR_max (in dB)	A_{eff_max} (in λ^2)	A_{eff_Total} (in λ^2)	Ω_max (in sr)	Ω_total (in sr)
Uniform	8; 1.2732	10.5253	0.8981	61.9326	1.1135	0.0161
DE	11.7825; 1.8752	12.0986	1.2902	60.2835	0.7751	0.0166
CRPSO	12.0543; 1.9185	12.1845	1.3160	57.3181	0.7599	0.0174
NPSO	10.5408; 1.6776	11.7913	1.2020	54.5211	0.8319	0.0183

Utilizing the modification described below leads to a significant enhancement in the global search capacity of the traditional PSO. This enhanced version of PSO is referred to as NPSO. NPSO technique is more efficient in global search, has few parameters to adjust, and has a high convergence speed compared to DE and CRPSO techniques.

To address this, instead of using independent r_1 and r_2 , a single random number, r_1 , is selected. By doing so, when r_1 is large, $(1 - r_1)$ is small and vice versa. However, to maintain control,

another random value, r_2 , is introduced. In certain exceptional situations, akin to fish schooling for food, after the particle's location has changed in accordance with Equation (12), a fish may not swim in the region it believes offers the best chance of finding food due to inertia. Alternatively, it may head in a direction opposing the expected prosperous regions. Therefore, in the subsequent step, the fish must adjust its travel direction to return to the promising area, and the presence of " $sign(r_3)$ " serves this purpose. Consequently, both the analytical and social components undergo modification,

where

$$\text{sign}(r_3) = \begin{cases} -1 & \text{when } r_3 \leq 0.05 \\ 1 & \text{when } r_3 > 0.05 \end{cases} \quad (13)$$

Ultimately, the enhanced velocity of the “ith” particle is formulated as [14].

$$V_i^{k+1} = r d_2 \times \text{sign}(r_3) \times V_i^k + (1 - r_2) \times c_1 \times r_1 \times (pb_i^k - X_i^k) + (1 - r_2) \times c_2 \times (1 - r_1) \times (gb_i^k - X_i^k) \quad (14)$$

The NPSO technique is implemented for the optimization of feeding current and inter-element spacing of CAA.

Numerical analysis and simulation results

In this section, the numerical outcomes of several CAA designs are described. The radiation pattern of CAA with the primary lobe pointed to $\phi_0 = 0^\circ$ is considered. It is assumed that there are six non-uniform CAAs with 10-, 12-, 16-, 20-, 36-, and 64-elements. The NPSO algorithm has been implemented with a population size of 120 and an iteration size of 400. The best-proven control parameter values of the NPSO technique have been discussed in Table 13. Optimized feed current and inter-element spacing with reduced SLL and improved FNBW are discussed below in test case 1, test case 2, test case 3, test case 4, test case 5, and test case 6 for 10-, 12-, 16-, 20-, 36-, and 64-element non-uniform CAA, respectively. Based on the simulation result, it is clear that the NPSO technique

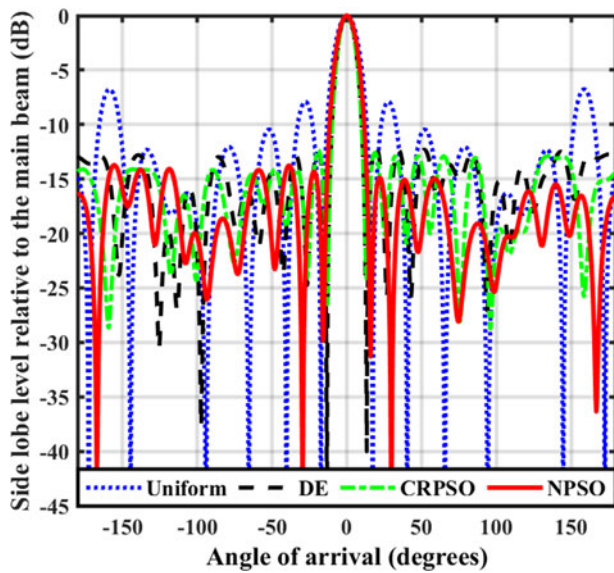


Figure 8. Radiation pattern of 16-element non-uniform CAAs.

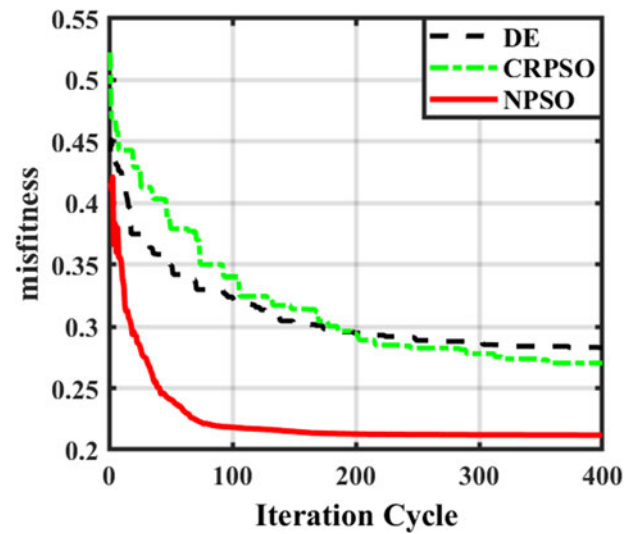


Figure 9. Convergence curve of 16-element non-uniform CAAs.

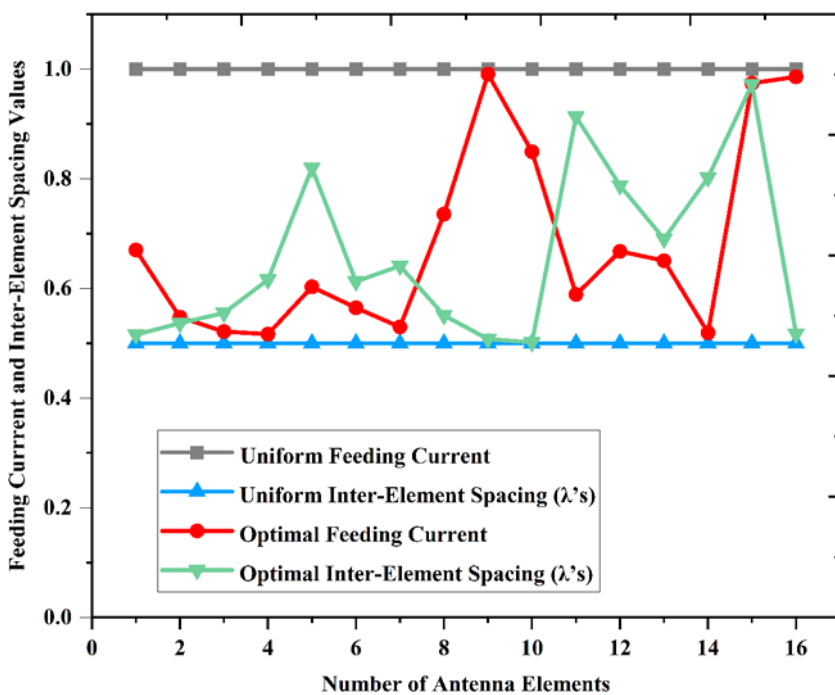


Figure 10. Optimal values of 16-element non-uniform CAAs using NPSO technique.

Table 7. Comparison of results obtained using the NPSO technique with other techniques for $N = 20$ elements

Algorithm	Optimal feeding current	Optimal inter-element spacing (in λ 's)	SLL (in dB)	FNBW (in degrees)
Uniform	1, 1, 1, 1, 1, 1, 1, 1, 1, 1, 1, 1, 1, 1, 1, 1, 1, 1, 1, 1	0.5, 0.5, 0.5, 0.5, 0.5, 0.5, 0.5, 0.5, 0.5, 0.5, 0.5, 0.5, 0.5, 0.5, 0.5, 0.5, 0.5, 0.5, 0.5, 0.5	-7.91	27.36
DE	0.9906, 0.6340, 0.6458, 0.5019, 0.5197, 0.5105, 0.6791, 0.7541, 0.7386, 0.9706, 0.6934, 0.7569, 0.6844, 0.5166, 0.5057, 0.5032, 0.8024, 0.6650, 0.9314, 0.9819	0.6055, 0.6885, 0.5271, 0.8963, 0.7660, 0.5636, 0.7920, 0.8631, 0.5840, 0.6567, 0.6916, 0.5744, 0.8807, 0.7436, 0.6857, 0.7365, 0.8925, 0.5955, 0.6053, 0.6244	-12.624	23.76
CRPSO	0.9463, 0.7525, 0.6387, 0.5169, 0.5029, 0.5015, 0.6498, 0.6966, 0.7566, 0.9923, 0.9322, 0.7060, 0.7997, 0.5009, 0.5036, 0.5004, 0.7192, 0.7572, 0.7407, 0.9898	0.6082, 0.6946, 0.7530, 0.8164, 0.6762, 0.6948, 0.9272, 0.5153, 0.5984, 0.5119, 0.6508, 0.5031, 0.9140, 0.8478, 0.7343, 0.7012, 0.7624, 0.8813, 0.5643, 0.6372	-13.695	23.04
NPSO	1.0000, 0.9620, 0.7113, 0.9964, 0.3900, 0.6050, 0.7669, 0.8747, 0.9684, 0.9848, 0.5532, 0.8391, 1.0000, 0.0667, 1.0000, 0.0001, 0.0000, 0.6498, 0.6638, 1.0000	0.5510, 0.5179, 0.9829, 0.7506, 0.6016, 0.7097, 0.9347, 0.9944, 0.5947, 0.7158, 0.5165, 0.6575, 0.5302, 0.8305, 0.5632, 0.6665, 0.9933, 0.5355, 0.6391, 0.7132	-14.770	26.28

Table 8. Other parameters' comparison using NPSO technique with different algorithms for $N = 20$ elements

Algorithm	$C; a$ (in λ 's)	DIR_max (in dB)	A_{eff_max} (in λ^2)	A_{eff_Total} (in λ^2)	Ω_{max} (in sr)	Ω_{total} (in sr)
Uniform	10; 1.5915	11.3105	1.0761	64.1195	0.9293	0.0156
DE	13.9730; 2.2239	12.7551	1.5007	55.8991	0.6664	0.0179
CRPSO	13.9924; 2.2270	12.8085	1.5193	55.5325	0.6582	0.0180
NPSO	13.9988; 2.2280	12.7064	1.4840	56.2097	0.6739	0.0178

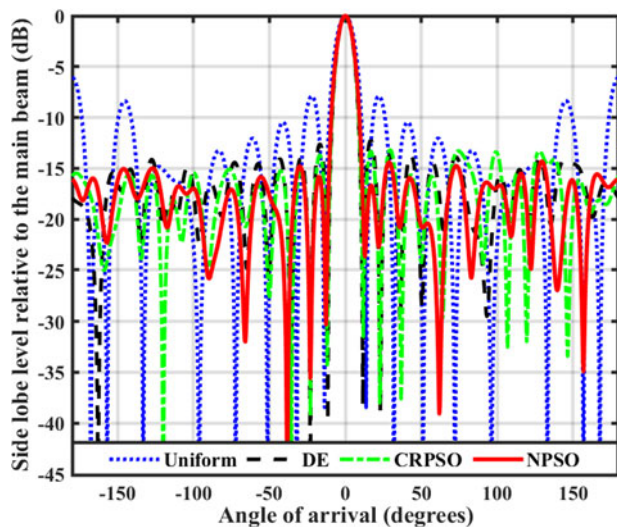


Figure 11. Radiation pattern of 20-element non-uniform CAAs.

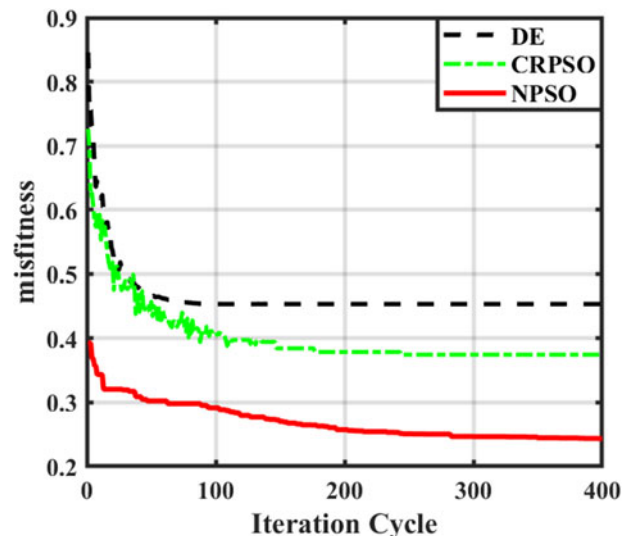


Figure 12. Convergence curve of 20-element non-uniform CAAs.

is more efficient in getting improved directivity, effective aperture, and beam area problems for implementation in an application with a wide range concerning DE, CRPSO, and previous work.

Test case 1: $N = 10$ elements

In test case 1, $N = 10$ elements of non-uniform CAAs have been considered. The DE, CRPSO, and NPSO techniques have been deployed to optimize excitation amplitude and inter-element spacing with low SLL and improved FNBW. From Table 1, it is clear that NPSO is outperforming concerning SLL of -14.140 dB as compared to uniform, DE, CRPSO, GA [8], SA [10], BBO [2],

SOA [12], PSO [9], OBA [27], and FA [28] with SLL of -7.93 dB, -11.204 dB, -11.810 dB, -9.811 dB, -13.00 dB, -13.95 dB, -12.83 dB, -12.307 dB, -14.06 dB, and -13.30 dB, respectively. NPSO is also outperforming concerning FNBW of 48.24° compared to uniform FNBW of 56.12°. After comparing these values with previously published results, it can be analyzed that the NPSO technique is more efficient in getting low SLL, improved directivity, and FNBW. Based on these optimized values, other parameters of CAAs can be calculated, as shown in Table 2. Figure 2 shows the radiation pattern with maximum SLL reduction and improved FNBW using DE, CRPSO, and NPSO. From Fig. 2, it is clear that maximum SLL was reduced using the NPSO technique as

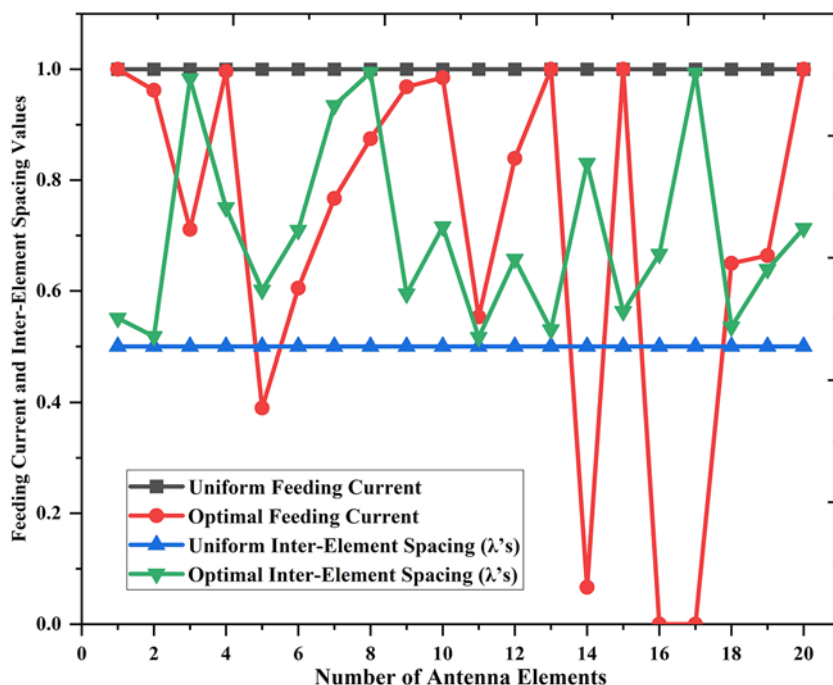


Figure 13. Optimal values of 20-element non-uniform CAAs using NPSO technique.

Table 9. Comparison of results obtained using the NPSO technique with other techniques for N = 36 elements

Algorithm	Optimal feeding current	Optimal inter-element spacing (in λ 's)	SLL (in dB)	FNBW (in degrees)
Uniform	1, 1	0.5, 0.5	-12.96	15.12
DE	1.0000, 0.7021, 0.9884, 0.8548, 0.3861, 0.4407, 0.0016, 0.5313, 0.6590, 0.3696, 0.3617, 0.0000, 0.0376, 1.0000, 0.4318, 1.0000, 0.7533, 0.9574, 0.3075, 0.7628, 0.9289, 0.3044, 0.3163, 0.3357, 0.6377, 0.1202, 0.5937, 0.0000, 0.2828, 0.2517, 1.0000, 0.6795, 0.7352, 0.2790, 0.7737, 0.9831	0.8090, 0.5976, 0.5779, 0.5620, 0.7981, 0.5641, 0.5273, 0.6460, 0.7261, 0.7765, 0.7744, 0.9324, 0.9126, 0.6828, 0.5846, 0.5861, 0.6624, 0.8514, 0.5322, 0.7345, 0.8676, 0.6859, 0.7244, 0.6099, 0.6631, 0.6761, 0.7324, 0.6747, 0.6554, 0.6220, 0.6101, 0.9205, 0.6314, 0.5020, 0.5919, 0.6271	-13.463	14.76
CRPSO	1.0000, 0.9969, 0.5958, 0.5903, 0.0000, 0.0000, 1.0000, 0.0000, 0.4906, 0.0021, 0.5204, 0.0683, 0.7928, 0.3761, 0.3118, 0.6898, 1.0000, 1.0000, 1.0000, 0.7422, 0.8009, 0.9893, 0.0064, 0.7001, 0.0001, 0.0000, 1.0000, 0.6062, 0.0094, 1.0000, 0.0000, 0.5347, 0.9063, 0.6866, 0.6460, 0.8755	0.6505, 0.6297, 0.6555, 0.8881, 0.5954, 0.6738, 0.5898, 0.6356, 0.8228, 0.6296, 0.6414, 0.5886, 0.6362, 0.7160, 0.7884, 0.9165, 0.5628, 0.7672, 0.7952, 0.6598, 0.5607, 0.5648, 0.7166, 0.8405, 0.5027, 0.6169, 0.7882, 0.8242, 0.9250, 0.8961, 0.6946, 0.8532, 0.6834, 0.5624, 0.5743, 0.6810	-14.381	13.68
NPSO	0.9407, 0.9571, 0.7874, 0.7558, 0.5504, 0.6508, 0.5485, 0.5022, 0.5559, 0.5207, 0.5597, 0.5739, 0.5352, 0.5947, 0.9162, 0.9262, 0.9401, 0.8686, 0.9687, 0.9092, 0.6601, 0.7255, 0.5707, 0.5071, 0.5215, 0.5502, 0.6744, 0.5074, 0.5769, 0.5952, 0.6922, 0.8507, 0.8434, 0.9124, 0.9917, 0.9391	0.6731, 0.5430, 0.5373, 0.5577, 0.7110, 0.9720, 0.6661, 0.8757, 0.8866, 0.7328, 0.7999, 0.7969, 0.7518, 0.7218, 0.6610, 0.5220, 0.6237, 0.6535, 0.6057, 0.5564, 0.5363, 0.8184, 0.9489, 0.7866, 0.8630, 0.6917, 0.7468, 0.6600, 0.7559, 0.7057, 0.9840, 0.5918, 0.5354, 0.5772, 0.5193, 0.5428	-15.145	12.96

Table 10. Other parameters' comparison using NPSO technique with different algorithms for N = 36 elements

Algorithm	C; a (in λ 's)	DIR_max (in dB)	A _{eff_max} (in λ^2)	A _{eff_Total} (in λ^2)	Ω _max (in sr)	Ω _total (in sr)
Uniform	18; 2.8648	13.3464	1.7196	62.2587	0.5815	0.0161
DE	24.6325; 3.9204	14.9203	2.4707	57.0030	0.4047	0.0175
CRPSO	25.1275; 3.9992	14.9356	2.4794	58.6577	0.4033	0.0170
NPSO	25.1118; 3.9967	15.0915	2.5700	57.1737	0.3891	0.0175

compared to DE and CRPSO techniques. Figure 3 shows the convergence curve using DE, CRPSO, and NPSO. From Fig. 3, it is clear that the NPSO technique is more efficient converges than the DE

and CRPSO techniques. Figure 4 shows the optimal values of feeding current and inter-element spacing of 10-element non-uniform CAAs using the NPSO technique.

Test case 2: $N = 12$ elements

In test case 2, $N = 12$ elements of non-uniform CAAs have been considered. The DE, CRPSO, and NPSO techniques have been deployed to optimize excitation amplitude and inter-element spacing with low SLL and improved FNBW. From Table 3, it is clear that NPSO is outperforming concerning SLL of -14.401 dB as compared to uniform, DE, CRPSO, GA [8], SA [10], BBO [2], SOA [12], PSO [9], OBA [27], and FA [28] with SLL of -7.90 dB, -11.610 dB, -13.130 dB, -11.830 dB, -13.910 dB, -13.95 dB, -13.77 dB, -13.670 dB, -14.30 dB, and -14.21 dB, respectively. NPSO is also outperforming concerning FNBW of 36.72° compared to uniform FNBW of 45.36° . After comparing these values with previously published results, it can be analyzed that the NPSO technique is more efficient in getting low SLL,

improved directivity, and FNBW. Based on these optimized values, other parameters of CAAs can be calculated, as shown in Table 4. Figure 5 shows the radiation pattern with maximum SLL reduction and improved FNBW using DE, CRPSO, and NPSO. From Fig. 5, it is clear that maximum SLL was reduced using the NPSO technique as compared to DE and CRPSO techniques. Figure 6 shows the convergence curve using DE, CRPSO, and NPSO. From Fig. 6, it is clear that the NPSO technique is more efficient and converges than the DE and CRPSO techniques. Figure 7 shows the optimal values of feeding current and inter-element spacing of 12-element non-uniform CAAs using the NPSO technique.

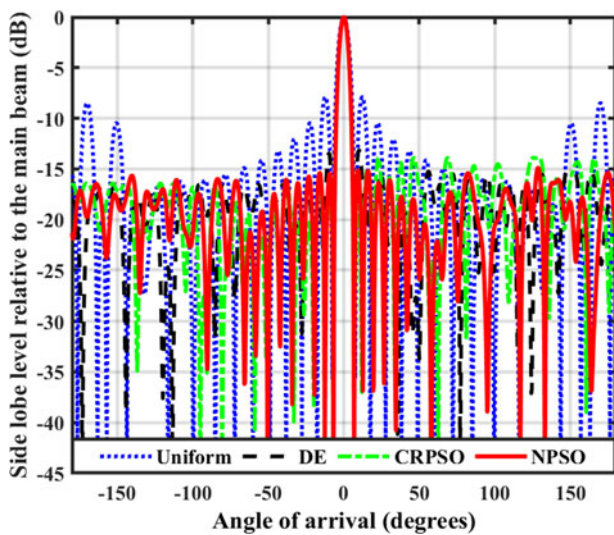


Figure 14. Radiation pattern of 36-element non-uniform CAAs.

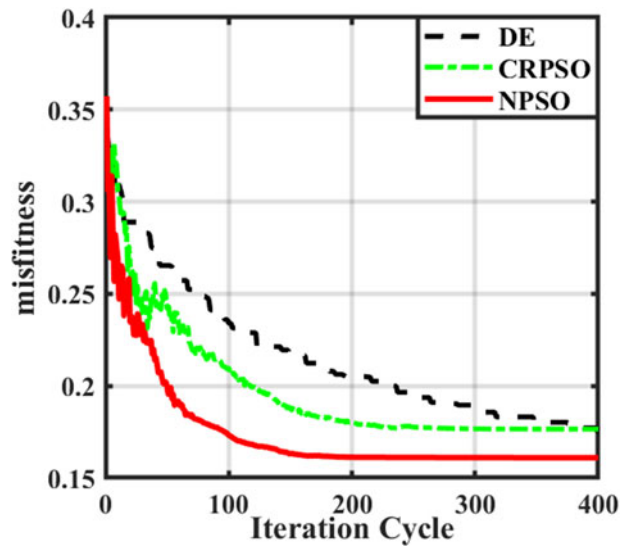


Figure 15. Convergence curve of 36-element non-uniform CAAs.

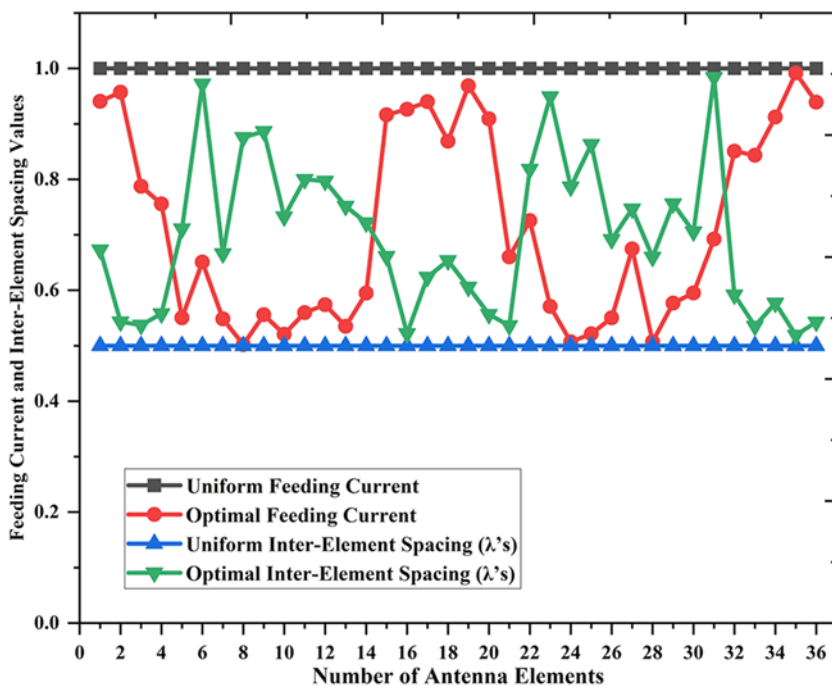


Figure 16. Optimal values of 36-element non-uniform CAAs using NPSO technique.

Test case 4: $N = 20$ elements

In test case 4, $N = 20$ elements of non-uniform CAAs have been considered. The DE, CRPSO, and NPSO techniques have been deployed to optimize excitation amplitude and inter-element spacing with low SLL and improved FNBW. From Table 7, it is clear that NPSO is outperforming concerning SLL of -14.770 dB as compared to uniform, DE, and CRPSO with SLL of -7.91 dB, -12.624 dB, and -13.695 dB, respectively. NPSO is also outperforming concerning FNBW of 26.28° compared to uniform FNBW of 27.36° . After comparing the NPSO's value with other values, it can be analyzed that the NPSO technique is more efficient in getting low SLL, improved directivity, and FNBW. Based on these optimized values, other parameters of CAAs can be calculated, as shown in Table 8. Figure 11 shows the radiation pattern

with maximum SLL reduction and improved FNBW using DE, CRPSO, and NPSO. From Fig. 11, it is clear that maximum SLL was reduced using the NPSO technique as compared to DE and CRPSO techniques. Figure 12 shows the convergence curve using DE, CRPSO, and NPSO. From Fig. 12, it is clear that the NPSO technique is more efficiently converged than the DE and CRPSO techniques. Figure 13 shows the optimal values of feeding current and inter-element spacing of 20-element non-uniform CAAs using the NPSO technique.

Test case 5: $N = 36$ elements

In test case 5, $N = 36$ elements of non-uniform CAAs have been considered. The DE, CRPSO, and NPSO techniques have been

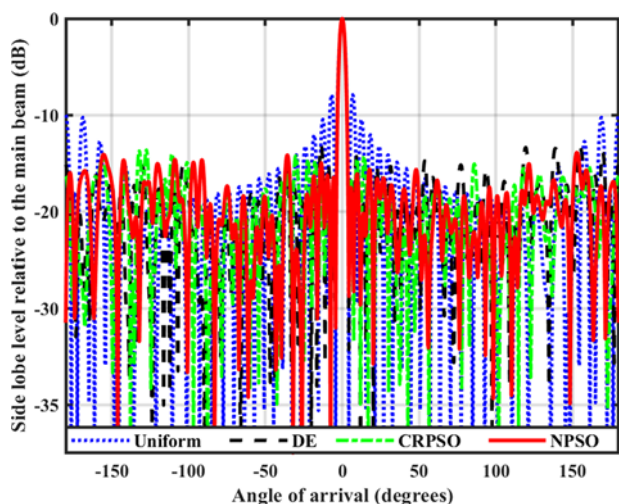


Figure 17. Radiation pattern of 64-element non-uniform CAAs.

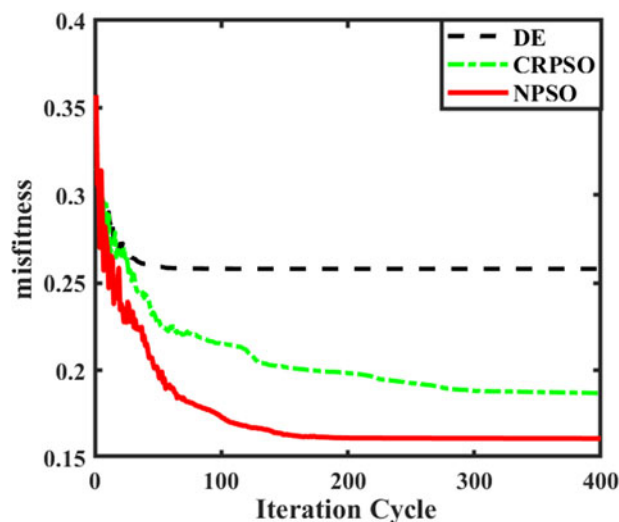


Figure 18. Convergence curve of 64-element non-uniform CAAs.

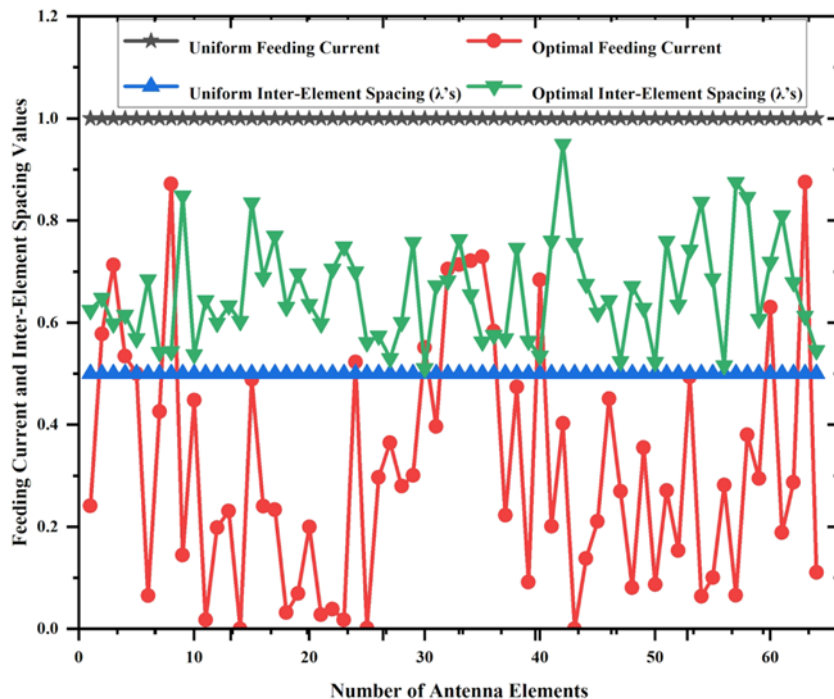


Figure 19. Optimal values of 64-element non-uniform CAAs using NPSO technique.

Table 13. Optimizing parameter of NPSO technique for N = 10-, 12-, 16-, 20-, 36, and 64-elements

Parameters	Values related to the number of elements in NPSO					
	10	12	16	20	36	64
Number of populations	120	120	120	120	120	120
Iteration size	400	400	400	400	400	400
$b_1 = b_2$	2.10	2.15	1.70	1.25	1.85	1.9
$W_1 = W_2 = W_3$ $= W_4 = W_5$	0.5	0.7	0.5	0.8	0.65	0.8

deployed to optimize excitation amplitude and inter-element spacing with low SLL and improved FNBW. From Table 9, it is clear that NPSO is outperforming concerning SLL of -15.145 dB as compared to uniform, DE, and CRPSO with SLL of -12.96 dB, -13.463 dB, and -14.381 dB, respectively. NPSO is also outperforming concerning FNBW of 12.96° compared to uniform, DE, and CRPSO with FNBW of 15.12° , 14.76° , and 13.68° , respectively. After comparing the NPSO's value with other values, it can be analyzed that the NPSO technique is more efficient in getting low SLL, improved directivity, and FNBW. Based on these optimized values, other parameters of CAAs can be calculated, as shown in Table 10. Figure 14 shows the radiation pattern with maximum SLL reduction and improved FNBW using DE, CRPSO, and NPSO. From Fig. 14, it is clear that maximum SLL was reduced using the NPSO technique as compared to DE and CRPSO techniques. Figure 15 shows the convergence curve using DE, CRPSO, and NPSO. From Fig. 15, it is clear that the NPSO technique is more efficient converges than the DE and CRPSO techniques. Figure 16 shows the optimal values of feeding current and inter-element spacing of 36-element non-uniform CAAs using the NPSO technique.

Test case 5: N = 64 elements

In test case 6, $N = 64$ elements of non-uniform CAAs have been considered. The DE, CRPSO, and NPSO techniques have been deployed to optimize excitation amplitude and inter-element spacing with low SLL and improved FNBW. From Table 11, it is clear that NPSO is outperforming concerning SLL of -16.105 dB as compared to uniform, DE, and CRPSO with SLL of -7.89 dB, -14.296 dB, and -14.743 dB, respectively. NPSO is also outperforming concerning FNBW of 8.64° compared to uniform, DE, and CRPSO with FNBW of 9.28° , 9.14° , and 9.00° , respectively. After comparing the NPSO's value with other values, it can be analyzed that the NPSO technique is more efficient in getting low SLL, improved directivity, and FNBW. Based on these optimized values, other parameters of CAAs can be calculated, as shown in Table 12. Figure 17 shows the radiation pattern with maximum SLL reduction and improved FNBW using DE, CRPSO, and NPSO. From Fig. 17, it is clear that maximum SLL was reduced using the NPSO technique as compared to DE and CRPSO techniques. Figure 18 shows the convergence curve using DE, CRPSO, and NPSO. From Fig. 18, it is clear that the NPSO technique is more efficiently converged than the DE and CRPSO techniques. Figure 19 shows the optimal values of feeding current and inter-element spacing of 64-element non-uniform CAAs using the NPSO technique.

Table 13 shows all optimizing parameter values for different antenna design problems using the NPSO technique.

Conclusion

Many applications may find circular arrays' relatively high SLLs unacceptable. Increased interference and a diminished capacity to distinguish between desired and unwanted signals can be caused by sidelobes. Because of their circular form, CAAs can be more challenging to design and optimize than linear arrays. Achieving the required radiation patterns may be difficult due to this intricacy, particularly when exact control over the SLLs and beam shape is needed. This article uses a meta-heuristic approach to discuss an unusual method of building antenna arrays. DE, CRPSO, and NPSO techniques have been deployed to get optimal feeding current and inter-element spacing with ultra-low SLL and improved FNBW. After analyzing the result, the NPSO technique is more efficient for different design problems of CAAs. For 10-, 12-, 16-, 20-, 36-, and 64-elements, a maximum reduction of SLL and improved FNBW can be obtained using the NPSO technique. Maximum directivity of the antenna array has been achieved. The circular design may limit the array's capacity to gather and transmit energy efficiently because it may result in a lower aperture efficiency when compared to alternative array layouts. The maximum effective aperture of the half-wave dipole antenna array is recorded as shown in test cases. The maximum beam area covered by the antenna array is shown in the table also. All these values are the best using the NPSO technique compared to other methods.

Further research will be planned to handle various geometry and constraints.

Acknowledgements. The authors want to thank the Government of India (GOI), SERB, and DST (Project Order No: EEQ/2021/000700; dated March 04, 2022) for giving the essential funds for this research.

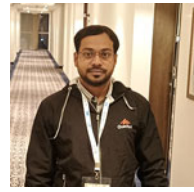
Competing interests. The authors report no conflict of interest.

References

- Blank SJ (1992) On the empirical optimization of antenna arrays. In *Adaptive Antenna Systems Symposium, Proceedings of the IEEE Long Island Section*, 13–16.
- Singh U and Kamal TS (2011) Design of non-uniform circular antenna arrays using biogeography-based optimization. *IET Microwaves, Antennas & Propagation* 5(11), 1365–1370.
- Güney K and Akdagh A (2001) Null steering of linear antenna arrays using a modified Tabu search algorithm. *Journal of Electromagnetic Waves and Applications* 15(7), 915–916.
- Elliott RS (2003) *Antenna Theory and Design (Revised)*. New Jersey: John Wiley.
- Dessouky MI, Sharshar HA and Albagory YA (2006) Efficient sidelobe reduction technique for small-sized concentric circular arrays. *Progress in Electromagnetics Research* 65, 187–200.
- Balanis CA (1997) *Antenna Theory Analysis and Design*, 2nd edn. New York: John Wiley and Son's Inc.
- Ram G, Mandal D, Ghoshal SP and Kar R (2013) IPSO-based performance comparison of optimum uniform and non-uniform spacing of circular antenna arrays. In *5th International Conference on Knowledge and Smart Technologies (KST)*, Burapha University.
- Panduro M, Mendez A, Dominguez R and Romero G (2006) Design of nonuniform antenna arrays for side lobe reduction using the method of genetic algorithm. *AEU – International Journal of Electronics and Communications* 60, 713–717.
- Mohammad S, Yahya N, Nihad D and Majid K (2008) Design of non-uniform circular antenna arrays using the particle swarm optimization. *Journal of Electrical Engineering* 59(9), 216–220.
- Rattan M, Patterh MS and Sohi BS (2009) Optimization of circular antenna arrays of isotropic radiators using simulated annealing.

International Journal of Microwave and Wireless Technologies 1(5), 441–446.

11. **Tabesh M, Kamyab M and Hakkak M** (2013) A circular array antenna design for radar applications. *IEEE Antennas and Wireless Propagation Letters* 12, 1028–1031.
12. **Ram G, Mandal D, Ghoshal SP and Kar R** (2013) Design of non-uniformly weighted and spaced circular antenna arrays with reduced side lobe level and first null beamwidth using a seeker optimization algorithm. In *International Conference on Swarm Evolutionary and Memetic Computing*, 35–46.
13. **Liu C** (2007) Circularly polarized microstrip antenna arrays for satellite communication. *IEEE Antennas and Wireless Propagation Letters* 6, 205–208.
14. **Reyna A, Panduro MA and Rio CD** (2011) Design of concentric ring antenna arrays for isoflux radiation in GEO satellites. *IEICE Electronics Express* 8(7), 484–490.
15. **Reyna A, Panduro M, Rio CD and Mendez AL** (2013) Design of concentric ring antenna arrays for a reconfigurable isoflux pattern. *Journal of Electromagnetic Waves and Applications*, 1–13.
16. **Ibarra M, Panduro M, Andrade AG and Reyna A** (2015) Design of sparse concentric rings array for LEO satellites. *Journal of Electromagnetic Waves and Applications* 29(15), 1983–2001.
17. **Ibarra M, Panduro M and Andrade AG** (2016) Differential evolution multi-objective for optimization of isoflux antenna arrays. *IETE Technical Review* 33(2), 105–114.
18. **Maldonado AR and Panduro M** (2014) Synthesis of concentric ring antenna array for a wide isoflux pattern. *International Journal of Numerical Modelling: Electronic Networks, Devices and Fields* 28, 433–441.
19. **Garza LA, Yepes LE, Covarrubias DH, Alonso MA and Panduro M** (2016) Synthesis of sparse circular antenna arrays applying a tapering technique over reconstructed continuous current distribution. *IET Microwaves, Antennas and Propagation* 10(3), 347–352.
20. **Bach H** (1970) Directivity of basic linear arrays. *IEEE Trans. Antennas Propagation Letters* 18, 107–110.
21. **Kraus JD** (1997) *Antennas*, 2nd edn. Tata McGraw-Hill.
22. **Panduro MA, Brizueta CA, Balderas LI and Acosta DA** (2009) A comparison of genetic algorithms, particle swarm optimization and the differential evolution method for the design of scannable circular antenna arrays. *Progress in Electromagnetics Research B* 13, 171–186.
23. **Kumar S, Ram G, Kar R and Mandal D** (2023) Analysis of feed network efficiency in time-modulated linear and circular array. In *IEEE Wireless Antenna and Microwave Symposium (WAMS)*.
24. **Panduro MA and Brizueta CA** (2008) Evolutionary multi-objective design of non-uniform circular phased arrays. *The International Journal for Computation and Mathematics in Electrical and Electronic Engineering* 27(2), 551–566.
25. **Mandal D, Ghoshal SP and Bhattacharjee AK** (2011) Wide null control of symmetric linear antenna array using novel particle swarm optimization. *International Journal of RF and Microwave Computer-Aided Engineering* 21, 376–382.
26. **Kumar S, Ram G, Kar R and Mandal D** (2022) Far field radiation pattern synthesis of circular antenna arrays using NPSO. In *2022 IEEE Microwaves, Antennas, and Propagation Conference (MAPCON)*, 676–680.
27. **Ram G, Mandal D, Ghoshal SP and Kar R** (2015) Opposition-based BAT algorithm for the optimal design of circular and concentric circular arrays with improved far-field radiation characteristics. *International Journal of Numerical Modelling: Electronic Networks, Devices and Fields* 24(2), 139–146.
28. **Sharaqa A and Dib N** (2014) Circular antenna array synthesis using firefly algorithm. *International Journal of RF and Microwave Computer-aided Engineering* 24(2), 139–146.



Satish Kumar (Member, IEEE) received the B.Tech. degree in electronics and communication engineering in 2013. He has received the M.Tech. degree in telecommunication engineering from the National Institute of Technology Durgapur, Durgapur, West Bengal, India, in 2018. In 2021, he joined as a full-time institute research scholar with the National Institute of Technology Durgapur to carry out research for his Ph.D. degree in the Department of Electronics and Communication Engineering. He has published six research papers at international and national conferences. His research interests include the analysis and synthesis of antenna arrays via bio-inspired evolutionary algorithms and antenna array optimization of various radiation characteristics.



Gopi Ram (Senior Member, IEEE) received the B.E. degree in electronics and telecommunication engineering from the Government Engineering College Jagdalpur, Jagdalpur, Chhattisgarh, India, in 2007, and the M.Tech. degree in telecommunication engineering from the National Institute of Technology Durgapur, Durgapur, West Bengal, India, in 2011. In 2012, he joined as a full-time institute research scholar with the National Institute of Technology Durgapur to carry out research for his Ph.D. degree. He received the scholarship from the Ministry of Human Resource and Development (MHRD), Government of India, from 2009 to 2011 (M.Tech. degree) and from 2012 to 2016 (Ph.D. degree). He joined NIT Warangal in April 2018, as an assistant professor with the Department of ECE, where he is currently working as an assistant professor with the Department of ECE. He has published more than 90 research papers in international journals and conferences. His research interests include analysis and synthesis of antenna arrays via bio-inspired evolutionary algorithms and antenna array optimization of various radiation characteristics.



Durbadal Mandal (Member, IEEE) received the B.E., M.Tech., and Ph.D. degrees from the National Institute of Technology, Durgapur, West Bengal, India. He is currently attached with the National Institute of Technology, Durgapur, as an associate professor with the Department of Electronics and Communication Engineering. He has published more than 400 research papers in international journals and conferences. He has produced 15+ Ph.D. students to date. His research interests include array antenna design and digital filter optimization via evolutionary optimization techniques.



Rajib Kar (Senior Member, IEEE) received the bachelor's degree in electronics and communication engineering from Regional Engineering College, Durgapur, West Bengal, India, in 2001, and the M.Tech. and Ph.D. degrees from the National Institute of Technology, Durgapur, West Bengal, India, in 2008 and 2011, respectively. Presently, he is attached to the National Institute of Technology, Durgapur, West Bengal, India, as an associate professor with the Department of Electronics and Communication Engineering. He has published more than 400 research papers in international journals and conferences. His research interests include very large-scale integrated circuit optimization and signal processing via evolutionary computing.